Journal of Thermal Analysis and Calorimetry, Vol. 70 (2002) 723–732

MELTING BEHAVIOR OF NYLON 6 FIBER IN TEXTILES

H. Kubokawa[1] *and T. Hatakeyama*[2*]

[1]Textile Research Institute of Gunma Prefecture, 5-46-1 Aioi-cho, Kiryu-shi 376-0011, Japan
[2]Otsuma Women's University, 12 Sanban-cho, Chiyoda-ku, Tokyo 102-8357, Japan

Abstract

The melting process of constrained nylon 6 fibers has been studied to estimate the true melting point of its original crystals. The melting peak became simpler in shape and shifted to higher temperature with increasing fiber-axis restricting force. When heating rate, β, was increased, the temperature where the melting curve initially departs from its baseline, T_{sm}, decreased steeply in the range of 45 to 60°C min^{-1}, and increased linearly with increasing β above 60°C min^{-1}. By linear extrapolation of T_{sm} to 0°C min^{-1}, the temperature of ca 190°C was obtained for the melting temperature of the original nylon 6 crystals. This seems to correspond to the zero-entropy-production melting of the most imperfect crystallites of the nylon 6 fabric.

Keywords: crystallization, double endotherm, DSC, multiple melting endotherm, nylon 6 fiber

Introduction

The molecular reorganization of fibrous polymers during heating has been investigated by many researchers in the last 40 years [1]. The DSC melting curves of semicrystalline fibers are altered by various factors, not only by their thermodynamically metastable nature but also by the macroscopic restricting force loaded on them. Semicrystalline fibers are scarcely constrained at a constant length although a weak restricting force remains. Textile structures generating a weak restricting force within samples are thought to be typical examples. Though the DSC analysis of textile samples is important for industrial purposes, DSC melting behavior has not been investigated in detail from a fundamental viewpoint.

The DSC melting behavior of the oriented polymers vary in a complex manner depending on heating conditions. Multiple endothermic peaks are often observed and moreover, endothermic peaks occasionally overlap. It is thought that the higher-order structure of molecular chains is frozen in the thermally non-equilibrium state and then rearranges in a wide temperature range of melting [1]. At the same time, the thermal gradient in the sample affects the DSC results. Thermal gradient depends not

* Author for correspondence: E-mail: hatakeyama@otsuma.ac.jp

1418–2874/2002/ $ 5.00

Akadémiai Kiadó, Budapest
Kluwer Academic Publishers, Dordrecht

only on the heat flow rate, but also thermal conductivity of polymers [2, 3]. It is considered that low thermal conductivity and direction dependency of thermal conductivity in oriented polymers [4] bring about the complex melting behavior.

Among a large number of oriented polymers, DSC melting behavior of nylon 6 and poly(ethylene terephtalate) (PET) fibers have received special attention due to industrial demand. The multiple melting behavior of many other polymers has been investigated and the melting–recrystallization–remelting mechanism of polymers on heating is now widely accepted [5–13].

As described above, polymers are in metastable states, and the reproducibility of their DSC data is diminished. Especially in the case of drawn fibers, it is known that the tensile force markedly affects their melting behavior. When Miyagi and Wunderlich [14] analyzed PET fibers by the constraining technique at a constant length using a differential thermal analyzer (DTA), the obtained melting peak was more simple in shape and higher in temperature in comparison with that measured by a standard technique. Todoki and Kawaguchi also studied the DSC melting peak of the nylon 6 fiber constrained at a constant length and obtained similar results [15]. In this study, nylon 6 fabrics were analyzed using a heat-flux DSC with various sample-packing methods and heating rates, in order to estimate the melting temperature of their original crystallites.

Experimental

Material

Nylon 6 fabric of the standard fabric for staining in the color fastness test [16] was used in this study: 70 denier fineness, 47 cm^{-1} warp density, 34 cm^{-1} weft density, plain weave, 70 g m^{-2} mass.

Differential scanning calorimetry (DSC)

The melting behavior of nylon 6 fabric was measured by using a differential scanning calorimeter (MAC Science Co., Ltd., DSC3200S). The temperature and enthalpy of DSC were calibrated by the standard materials of indium, tin, lead and zinc, whose purity is ≥99.999%. Samples were packed in open-type aluminium sample pans by the following four techniques. In technique 1, a sample fabric was cut into a disc of 4-mm diameter and packed in a sample vessel. In technique 2, a short cut sample was unraveled to short fibers and packed in a vessel. In technique 3, warp and weft fibers unraveled from the sample fabric were wound around a thin aluminium cover disc to be constrained at a constant length and packed in a vessel. The mass ratio of the warp and the weft was adjusted to that of the fabric. In technique 4, a fine copper powder of ca 30 mg was added to a cut sample to fill up an opening within the sample and packed densely in a vessel, in order to increase the thermal conductivity [17]. Sample mass was ca 0.9 or 4.5 mg, which corresponded to 5-sheet samples prepared by techniques 1 or 4. The measurements were performed in an atmosphere of nitrogen at 50 mL min^{-1}, at various heating rates from 10 to 100°C min^{-1}.

Results and discussion

Figure 1 shows the DSC curves of the samples (ca 0.9 mg) packed by techniques 1, 2 and 3 measured at 10°C min^{-1}. Double endotherms are observed in the DSC curve of the sample packed by technique 1. The DSC pattern is similar to that reported by Todoki and Kawaguchi [5], and suggests that the partial melting and reorganization of crystallites occurs in the heating process. On the other hand, triple endotherms are observed in the melting curve by technique 2. The total position of the endothermic change slightly shifts to the low-temperature side in comparison with that of technique 1. In the case of technique 3, the melting peak is simpler in shape and shifts to higher temperature. This result agrees with that reported by Todoki and Kawaguchi [15]. In the initial stage of melting, step-like shoulder peaks are observed, suggesting that the ends of fibers, which were not constrained, melted at the lower temperatures in comparison with the constrained parts. As the fiber-restricting force is expected to increase in the order of technique 2, 1 and 3, the above tendency in the change of the melting curve is thought to be reasonable.

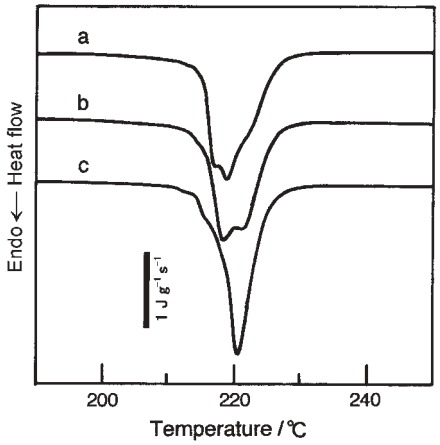

Fig. 1 DSC heating curves measured at 10°C min^{-1} of the variously-packed nylon 6 fabrics. Curves a, b and c show those of samples packed by techniques 2, 1 and 3, respectively

Concerning the mechanism in which the restricting force along the fiber-axis affects the melting behavior of semicrystalline fiber, the following explanations were proposed. Miyagi and Wunderlich [14] concluded that the shift of melting peak to higher temperature, which was observed in the DSC curve of the constrained PET fiber, results from a temporary entropic restriction, as described by Zachmann [18]. Todoki and Kawaguchi [15, 19] proposed based on the theoretical studies investigated by Zachmann and Spelluci [20, 21] that the networks of residual crystallites connected by tie molecules play the same role as cross-links of elongated rubber [22] to shift the melting peak to higher temperature. This network model of crystallites seems to be reasonable because the restricting force generated by techniques 1 or 3 is transmitted through the network. This transmitted force is supposed to reduce the

thermodynamic fluctuations, which are considered as the driving force of fusion, around the interfaces between crystallites and amorphous regions. Therefore, it is suggested that the reduction of fluctuations controls their partial melting to change the melting-recrystallization-remelting behavior.

The melting enthalpy of ca 75.7 J g^{-1} was estimated from the peak area in Fig. 1. The enthalpy of melting was not affected by the difference in strength of restricting force, even if the melting-recrystallization-remelting behavior is observed in a different manner in DSC curves.

The 5-sheet sample of ca 4.5 mg packed by technique 1 was measured at 10°C min^{-1}. The DSC curve and its time-differentiated curve are shown in Fig. 2, together with those of the 1-sheet sample. As shown in Fig. 2, the multiple melting behavior of the 5-sheet sample is not clear, and the peaks shifted to higher temperature in comparison with those of the 1-sheet sample. In addition, the melting enthalpy was estimated at 74.9 J g^{-1}, which was smaller than the 1-sheet sample.

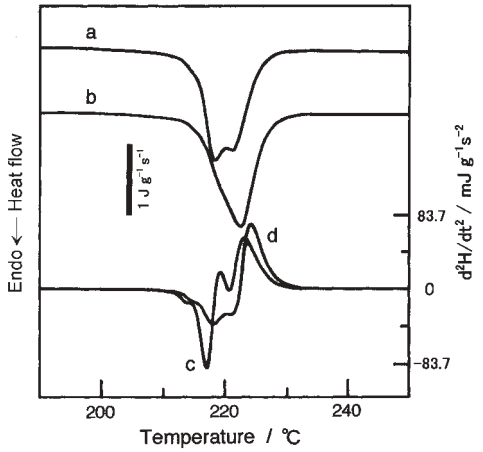

Fig. 2 DSC heating curves measured at 10°C min^{-1} of the 1-sheet and 5-sheet samples of nylon 6 fabric packed by technique 1, and their time-differentiated curves. Curves a and c show the DSC curve and its time-differentiated one of 1-sheet sample, respectively. Similarly, curves b and d show those of 5-sheet samples

This difference in melting behavior is attributed to the temperature gradient within a sample because the air included in the 5-sheet sample may reduce the thermal conductivity considerably. As shown in Fig. 3, when the 1-sheet and 5-sheet samples were packed by technique 4, both melting peaks are sharp and apparently single, and the peak temperature shifts to higher temperature in comparison with that of the 1-sheet sample in Fig. 2. Moreover, both their melting enthalpies were ca 75.7 J g^{-1}. The results strongly indicate that the DSC curve is affected by the thermal gradient within the sample.

The temperature gradient within the samples is thought to decrease in the presence of copper powder. Considering the changes in their DSC curves, however, the addition of copper powder seems to cause another melting-recrystallization-remelting route during

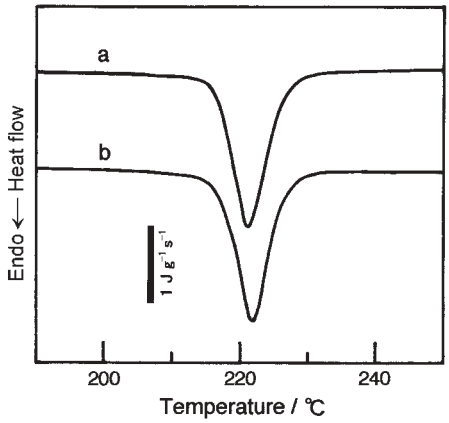

Fig. 3 DSC heating curves measured at 10°C min^{-1} of the nylon 6 fabrics packed by technique 4. Curves a and b show those of 1-sheet and 5-sheet samples, respectively

the melting of the nylon 6 fiber. As with the sample packed by technique 3, these changes are thought to result from the increase of restricting force, which was caused by densely packing with a fine copper powder. The melting behavior of semicrystalline fiber is strongly affected by the restricting force, and moreover, directly reflects its uneven state, as observed in curve (c) of Fig. 1. Therefore, it is important to keep the restricting force at a constant level in order to obtain reliable data.

In the case of measurement at 10°C min^{-1}, as described above, all the melting enthalpies of the samples packed in different ways were identical, except for that of the 5-sheet sample packed by technique 1. However, this result does not suggest that their original crystallites have been maintained before melting. In the heating process before melting, the crystallites are thought to become a more perfect crystalline form, even if little trace is observed in the DSC curve. Miyagi and Wunderlich heated PET fibers in a rapid heating rate by DTA in order to transform directly from the metastable crystals to the metastable melt of the same free energy, which was called zero-entropy-production melting [14]. For the same purpose, the nylon 6 fabrics were measured at high heating rates.

Before the investigation of the nylon 6 fiber, the heating rate dependency of the melting behavior of indium, a standard material, was examined as follows. While T_{im} (an initial temperature) and T_{pm} (a peak temperature) shown in Fig. 4 are usually determined as melting temperatures in DSC curves, the T_{sm} temperature where the melting curve initially departs from its baseline, was further used in this study. When indium of 4.98 mg was measured at various heating rates from 3 to 100°C min^{-1}, the obtained relationships between the melting temperatures of T_{sm}, T_{im} and T_{pm} and heating rates are shown in Fig. 5. In this figure, it is shown that T_{sm}, T_{im} and T_{pm} increased with increasing heating rate. According to the strict solution [23, 24] based on the theoretical model for a heat-flux DSC investigated by Mraw [25], only T_{sm} is related to the real melting temperature (T_{fus}) among the above melting temperatures. The relationship between T_{fus} and T_{sm} is given as

$$T_{fus}=T_{sm}-CR\beta \quad (1)$$

where C is the heat capacity of the sample material itself and its vessel, R is the thermal resistance between the sample-temperature monitoring station and the sample itself and β is the heating rate.

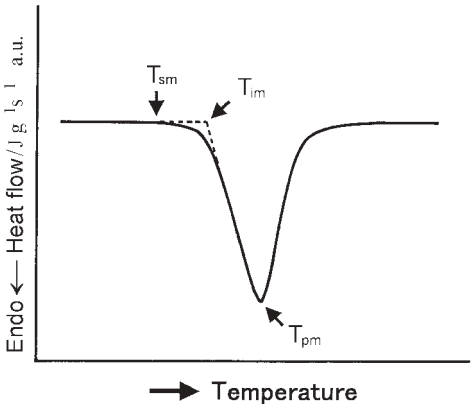

Fig. 4 Illustration of T_{sm}, T_{im} and T_{pm} in a DSC melting curve

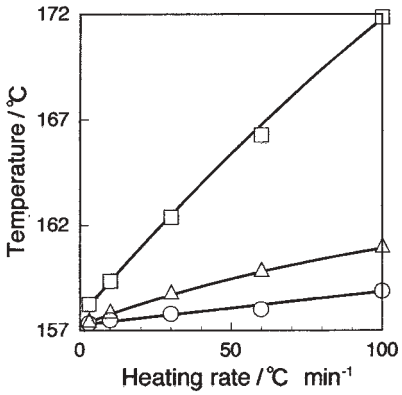

Fig. 5 Relationships between the melting temperatures of o – T_{sm}, △ – T_{im} and □ – T_{pm} and heating rates, when the DSC heating curves of indium were measured at various heating rates from 3 to 100°C min^{-1}

This equation suggests that the slope of the straight line drawn through T_{sm} *vs*. β plots is given by CR and T_{sm} is higher than T_{fus} by $CR\beta$. For example, T_{sm} of indium measured at 100°C min^{-1} was thought to be higher than T_{fus} by ca 1.55°C. In addition, this analytical technique is adaptable for power compensation DSC, since Eq. (1) is valid too [24].

Figure 6 shows the melting behavior of nylon 6 fibers of ca 0.9 mg packed by technique 1 at various heating rates from 10 to 100°C min^{-1}. The relationships between the melting temperatures of T_{sm}, T_{im} and T_{pm} and heating rates are obtained in

Fig. 7. T_{sm} was determined as the temperature where the time-differentiated DSC data started decreasing discontinuously, because a slight change of endotherm was difficult to detect at the start of melting on the DSC curve. In Fig. 7, T_{pm} increases with increasing heating rate and T_{im} slightly increases. On the other hand, T_{sm} depends on heating rate in a different manner. T_{sm} remains constant at 205°C up to 45°C min^{-1} and then decreases steeply in the range of 45 to 60°C min^{-1}, and then increases linearly with heating rate above 60°C min^{-1}. The heating-rate dependency of T_{sm} was confirmed with a good reproducibility. In order to improve the accuracy of T_{sm} values, they were determined in a definite procedure based on the time-differentiated DSC data. In this procedure, T_{sm} values could be obtained with personal errors of less than 1 degree. Improvement of detection sensitivity and normalization of T_{sm} determination are important to minimize personal errors.

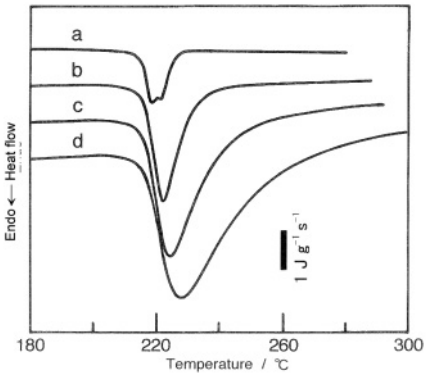

Fig. 6 DSC heating curves measured at various heating rates from 10 to 100°C min^{-1} of nylon 6 fabrics packed by technique 1: a – 10, b – 30, c – 60 and d – 100°C min^{-1}

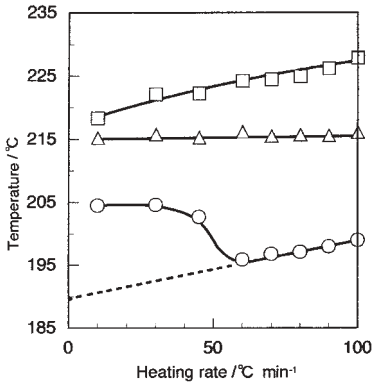

Fig. 7 Relationships between the melting temperatures of o – T_{sm}, △ – T_{im} and □ – T_{pm} and heating rates, when the DSC heating curves of nylon 6 fabrics packed by technique 1 were measured at various heating rates from 10 to 100°C min^{-1}

In the time-differentiated DSC curves measured at the heating rates lower than 45°C min^{-1}, a slight exothermic change due to premelt-crystallization was observed, but the exothermic change was not observed at the heating rates higher than 60°C min^{-1}. The exothermic change disappeared in the range of 45 to 60°C min^{-1}. The above results indicate that the premelt-crystallization is inhibited by high-speed heating. Therefore, the shift of T_{sm} to lower temperature is attributed to no reorganization of the crystallites.

The T_{sm} values at the heating rates lower than 45°C min^{-1} correspond to the temperature where premelt-crystallization is terminated. On this account, the T_{sm}–β relation is discontinuous at the heating rates between 45 and 60°C min^{-1}. On the other hand, the linear increase of T_{sm} in the β range of 60 to 100°C min^{-1} is thought to be attributed to $CR\beta$ in Eq. (1). The slope of the straight line drawn through the plots of T_{sm}–β for nylon 6 is almost 6 times larger than that of indium. It is reasonable to consider that the difference in slope, or CR, comes from their heat capacity difference.

As described above, the premelt-crystallization of the nylon 6 fiber was not observed at a heating rate of larger than 60°C min^{-1}. Wunderlich reported that the zero-entropy-production melting of thin, lamellar polyethylene crystals could be established at a heating rate higher than 50°C min^{-1} [26]. If the reorganization of the crystallites is thoroughly inhibited by the high-speed heating higher than 60°C min^{-1}, the temperature estimated by extrapolation of the linear T_{sm}–β relation to 0°C min^{-1} corresponds to that of zero-entropy-production melting. Considering the fact that there exists a distribution of sizes among the crystallites, the estimated temperature is thought to correspond to that of the smallest, or most imperfect, crystallites. The estimated temperature by extrapolation in Fig. 7 was ca 190°C.

Todoki and Kawaguchi measured the melting behavior of the irradiated nylon 6 fiber in which the amorphous regions were cross-linked selectively via amide groups with acetylene as a pretreatment. They estimated that the temperature of zero-entropy-production melting is 190°C [27, 28]. Though there are several differences in sample and conditions, both the results are agreed quite well.

The temperature of zero-entropy-production melting is thought to be a characteristic physical property corresponding to the imperfect state of the nylon 6 fibers, because the crystallites melt maintaining their original imperfection. On the other hand, T_{im} and T_{pm} appear in a DSC melting curve as the results of the competition between melting and reorganization of crystallites, and are not related with T_{fus}. They reflect the total results of nucleation and nuclear growth in melting and crystallization, which are affected by numerous factors, such as restricting force, heating rate, and so on.

Determination of the melting enthalpies at high heating rates is described below. In the case of indium, the area of the melting peak became smaller in proportion to the heating rate. On the other hand, the peak of the nylon 6 fabric became greater and broader with increasing heating rate, as shown in Fig. 6. Since a stable baseline was not obtained, the melting enthalpies could not be determined at high heating rates.

Conclusions

A new viewpoint was provided for understanding a complex melting behavior of semicrystalline fiber by the attempt to relate the experimental data of melting temperature to the mathematical theory for DSC. In the case of the DSC measurement of melting of drawn fibers, it was suggested that the fiber-restricting force changes the melting-recrystallization-remelting behavior of fiber. T_{im} and T_{pm} were considered as the results of the competition between melting and reorganization of crystallites. They reflect the total results of nucleation and growth in melting and crystallization, which are affected by numerous factors, such as restricting force and heating rate, etc. The temperature estimated by extrapolation of the linear T_{sm}–β relation to 0°C min^{-1} corresponds to that of the zero-entropy-production melting of the smallest crystallites. This temperature is supposed to be a true melting temperature characteristic of an imperfect state of drawn fiber, because the crystallites melt maintaining their original imperfection.

* * *

We wish to thank Dr. Shigeo Hirose, National Institute of Advanced Industrial Science and Technology and Professor Clive Langham for their helpful comments.

References

1 B. Wunderlich; Ed. E. A. Turi, 'Thermal Characterization of Polymeric Materials', Academic Press, San Diego 1997, Chapter 2.
2 S. Ichihara, Netsu-Sokutei, 3 (1976) 83.
3 T. Hatakeyama and F. X. Quinn, 'Thermal Analysis: Fundamentals and Applications to Polymer Science', John Wiley & Sons, Chichester 1994, p. 25.
4 T. Hatakeyama and L. Zhenhai, 'Handbook of Thermal Analysis', John Wiley & Sons, Chichester 1998, p. 102.
5 M. Todoki and T. Kawaguchi, J. Polym. Sci. Polym. Phys. Ed., 15 (1977) 1067.
6 R. A. Phillips, J. Polym. Sci. Polym. Phys. Ed., 36 (1998) 495.
7 H. G. Kim and R. E. Robertson, J. Polym. Sci. Polym. Phys. Ed., 36 (1998) 1757.
8 E. S. Yoo and S. S. Im, J. Polym. Sci. Polym. Phys. Ed., 37 (1999) 1357.
9 C. S. Wang and C. H. Lin, J. Polym. Sci. Polym. Phys. Ed., 37 (1999) 2269.
10 R. A. Phillips and R. L. Jones, Macromol. Chem. Phys., 200 (1999) 1912.
11 P. Supaphol and J. E. Spruiell, J. Appl. Polym. Sci., 75 (2000) 44.
12 X. Zhu, D. Yan, S. Tan, T. Wang, D. Yan and E. Zhou, J. Appl. Polym. Sci., 77 (2000) 163.
13 T. M. Wu, C. C. Chang and T. L. Yu, J. Polym. Sci. Polym. Phys. Ed., 38 (2000) 2515.
14 A. Miyagi and B. Wunderlich, J. Polym. Sci. Polym. Phys. Ed., 10 (1972) 1401.
15 M. Todoki and T. Kawaguchi, J. Polym. Sci. Polym. Phys. Ed., 15 (1977) 1507.
16 Japanese Industrial Standards Committee, 'Standard Adjacent Fabrics for Staining of Colour Fastness Test (JIS L 0803)', Japan Standards Association, 1992.
17 T. Hatakeyama, H. Yoshida, C. Nagasaki and H. Hatakeyama, Polymer, 17 (1976) 559.
18 H. G. Zachmann, Kolloid-Z. Z. Polym., 206 (1965) 25.
19 T. Kawaguchi and M. Todoki, Sen'I Gakkaishi, 34 (1978) 11.
20 H. G. Zachmann and P. Spelluci, Kolloid-Z. Z. Polym., 213 (1966) 39.

21 H. G. Zachmann, Kolloid-Z. Z. Polym., 231 (1969) 504.
22 P. J. Flory, 'Principles of Polymer Chemistry', Cornell University Press, Ithaca, New York 1953, Chapter 11.
23 Y. Saito, K. Saito and T. Atake, Thermochim. Acta, 99 (1986) 299.
24 K. Saito, T. Atake and Y. Saito, Netsu-Sokutei, 14 (1987) 2.
25 S. C. Mraw, Rev. Sci. Instrum., 53 (1982) 228.
26 B. Wunderlich, 'Thermal Analysis', Academic Press, San Diego, 1990, p. 197.
27 M. Todoki and T. Kawaguchi, Kobunshi Ronbunshu, 31 (1974) 106.
28 M. Todoki and T. Kawaguchi, Kobunshi Ronbunshu, 32 (1975) 363.